frontiers in Physics

ORIGINAL RESEARCH
published: 11 February 2020
doi: 10.3389/fphy.2020.00021

Study of the Cumulative Dose Between Fractions of Lung Cancer Radiotherapy Based on CT and CBCT Image Deformable Registration Technology

Judong Luo[1], *Changdong Ma*[2], *Shuang Yu*[2], *Zhenjiang Li*[3] *and Changsheng Ma*[3]*

[1] Department of Oncology, The Affiliated Changzhou No.2 People's Hospital of Nanjing Medical University, Changzhou, China, [2] Department of Radiation Therapy, Qilu Hospital of Shandong University, Jinan, China, [3] Department of Radiotherapy, Shandong Cancer Hospital and Institute, Shandong First Medical University and Shandong Academy of Medical Sciences, Jinan, China

OPEN ACCESS

Edited by:
Andreas Hess,
Friedrich-Alexander University Erlangen-Nürnberg, Germany

Reviewed by:
Wazir Muhammad,
Yale University, United States
Fei Geng,
McMaster University, Canada

***Correspondence:**
Changsheng Ma
machangsheng_2000@126.com

Specialty section:
This article was submitted to Medical Physics and Imaging, a section of the journal Frontiers in Physics

Received: 15 July 2019
Accepted: 24 January 2020
Published: 11 February 2020

Citation:
Luo J, Ma C, Yu S, Li Z and Ma C (2020) Study of the Cumulative Dose Between Fractions of Lung Cancer Radiotherapy Based on CT and CBCT Image Deformable Registration Technology. Front. Phys. 8:21. doi: 10.3389/fphy.2020.00021

Objective: To analyze the difference between planned dose and delivered dose by accumulating the dose based on CT and CBCT image deformable registration.

Methods: The clinical data of 24 NSCLC (non-small cell lung cancer) patients receiving conformal radiotherapy or intensity-modulated radiotherapy (IMRT) were retrospectively analyzed. With the CBCT image of each week as the target image, we performed the deformation registration for CBCT images and planning CT images in RayStation. The delivered dose of CBCT images compared to the planning CT images was accumulated with the use of mapping relationships in registration. The differences in planned dose and accumulative dose of target and at-risk organs were compared.

Results: The average planned and accumulative doses of GTV in 24 patients were 5832.45 ± 645.42 and 5750.65 ± 630.27 cGy, respectively ($P < 0.05$). The average planning target volume (PTV) in CT plans and accumulation plans reaching the prescription dose was 95.59 and 81.47% of the PTV ($P > 0.05$). At the stage of treatment, the volumes of the at-risk organs in CBCT images were not significantly different. There were no statistically significant differences in the probability of complications in the right lung, left lung, heart, total lung, or spinal cord ($P > 0.05$).

Conclusion: With the dose deformable registration method, the dose caused by changes in the target anatomical structure of NSCLC patients was found. The dose to organs did not change much. However, in some patients, the received radiation in the target organ was less than the prescribed dose.

Keywords: non-small cell lung cancer, dose-volume histogram, fraction delivered dose, deformable registration, accumulative dose

INTRODUCTION

In current radiotherapy practice IMRT technology can significantly improve the rate of tumor control and reduce complications. Therefore, IMRT is widely used in some complex target radiotherapies [1]. Multiple factors can affect the precise implementation of radiotherapy. There will be changes in the location of the target for each radiotherapy fraction, which can lead to difference between the planned dose and cumulative dose. For example, a target volume reduction will lead to bad dose distribution, and the surrounding normal tissue into the high dose area can increase the normal tissue radiation dose [2]. Therefore, it is necessary to analyze these changes during the process of fraction radiotherapy.

Adaptive radiation therapy (ART) is based on image data, cumulative dose, and other dose information to understand the various changes in patients, make timely adjustments to the planning target volume (PTV) and clinical target volume (CTV), and modify the prescribed dose and treatment plan to improve follow-up treatment and more accurately apply radiation therapy. Generally speaking, image-guided radiotherapy, volume-guided radiotherapy, and dose-guided radiotherapy are part of ART [3]. In this study, we analyzed the difference between planned dose and delivered dose by calculating the accumulated dose based on deformable registration, and we analyzed the changes in the volume and dose of targets and organs-at-risk by comparing cone beam CT (CBCT) images and planning CT images of patients with non-small cell lung cancer (NSCLC). We initially studied the actual dose volume histogram of target and OARs in NSCLC radiotherapy.

MATERIALS AND METHODS

Plan CT Acquisition and Target Contour

A total of 24 patients with NSCLC who underwent CRT or IMRT (24 sets of CT images and CBCT images) were retrospectively analyzed from January 2014 to January 2015 in Shandong Tumor Hospital. 18 patients were male, and the others were female. The median age was 58 years (range, 47–65 years). General clinical data of patients were as shown in **Table 1**. The pCT was obtained with a fan-beam helical CT scanner (Philips Brilliance Big Bore 16 slice CT, Philips Medical Systems, Eindhoven, The Netherlands) with 3 mm slice thickness and 512 × 512 pixels. The pCT was imported into the RayStation radiotherapy planning system via the network. The target and OARs were contoured on pCT. The target of radiotherapy included the gross tumor target (GTV), the clinical target (CTV) with the small lesion, the inner target (ITV) edge of the target movement, and the margin of the PTV. When the lung cancer target was outlined, the width and window position of the CT window were 1,600 and −600 HU, respectively, and the window width and window position of the Mediastinum window were 400 and 20 HU, respectively. Unless, there was evidence of invasion, CTV should not have exceeded the anatomical range. The lung cancer primary tumor was GTV + (6 ∼ 8) mm + respiratory mobility + setup error. The mediastinal lymph node was PTV for GTV + (3 ∼ 5) mm + respiratory mobility + setup error. The doctor could base the dose on the normal structure around the target to modify it as appropriate. The OARs included the lungs, spinal cord, heart, and esophagus.

TABLE 1 | General clinical data of patients.

Characteristics	Value
Gender	
Male	18
Female	6
Age	47–65 y, median 58
Stage	
IIIA	14
IIIB	10
Squamous	16
Adenocarcinoma	8
GTV/cm^3	17.6 ± 8.1 cm^3 Range (8.69–36.58)
PTV/cm^3	98.59 ± 30.27 cm^3 Range (744.65–2197.43)
Left lung/cm^3	1355.52 ± 744.65 cm^3 Range (744.65–2197.43)
Right lung/cm3	1738.77 ± 890.12 cm^3 Range (1047.76–2424.55)

The Radiotherapy Plan Design

The physicians used the RayStation treatment planning system, and the conformal plans generally included a 6 MV X-ray and 4–6 fixed conformal fields. The lateral angle was adjusted as far as possible to make its long axis parallel to the target, reducing the volume through the lung tissue, to ensure that at least one field completely avoided the spinal cord, and all the field angle intervals should have been as high as 40°. It was common to have 5 fields for lung tumors. Conventional IMRTs typically consisted of 5–7 fields, and the separation angles were the same. When IMRT was applied to lung cancer, the number of fields and the angle separation tended to be adjusted according to the actual situation. The prescription dose was 2.0 Gy × 30 fractions; V30 < 20% or average lung dose (Dmean) ≤ 20 Gy; heart V30 ≤ 46% or Dmean <26 Gy; esophageal V50 ≤ 30% or Dmean ≤ (34 ∼ 40) Gy, maximum dose (Dmax) ≤ (58 ∼ 74) Gy.

CBCT Image Acquisition

Twenty-four patients underwent CBCT scanning before treatment. According to the scanning range, the reference center level was selected. In the three-dimensional laser light, the front and the left and right sides of the center of the body were marked. The Elekta Synergy (Elekta Oncology Systems, Crawley, UK) accelerator XVI system acquired the CBCT images. The system consists of a high-level X-ray tube and a large, amorphous silicon X-ray detection board through the telescopic robot arm installed on both sides of the linear accelerator rack. The scan mode was half-phan mode, and the rotation angle was 200°. The scanning parameters were as follows: tube voltage 120 kV, tube current 25 mA, acquisition rate 5.5 frames/s, plus bowtie filter, and S20 collimator. The process of XVI acquisition was issued by the tube pulsed X-ray (frequency fixed to 5.75 Hz). The radiation went through the scanning object, and then the signal was read and stored by the plate detector. The above process was repeated to collect data. The image reconstruction matrix was 512 × 512, the

reconstructed layer thickness was 3 mm, and the CBCT image was 88 layers. The CBCT scan was done once every time the patient was treated, and the image registration and the setup error were corrected. Finally, all CT and CBCT images were imported into the RayStation treatment planning system.

CT and CBCT Image Deformable Registration

CBCT image targets and OARs were outlined by the function of automatic profiling in the RayStation treatment planning system. The outlines were then manually corrected by the clinicians. The CT image was used as the reference image, and the daily CBCT image was used as the target image. The rigid registration was based on the outer contour of the body, and then the deformation registration was applied based on the gray-value information. If necessary, we manually modified the result of the rigid registration. We applied the target mapping to the planned CT target and OAR to the CBCT image.

CBCT Fractional Dose Calculation and Accumulation

Using dose tracking and cumulative doses in the Adaptive Radiation module in the RayStation treatment planning system, the individual CBCT electronic density tables obtained from each patient's CT image map were selected for CBCT images. Based on the CBCT image, the fractional dose was calculated, and the fractional dose was added to the planned CT image to obtain the cumulative dose.

Normal Tissue Complication Probability (NTCP)

Normal tissue complication probability (NTCP) values were also calculated for each OAR with the Lyman-Kutcher-Burman (LKB) model. The three parameters were derived according to Burman identification: several parameters, including mean hepatic dose, percentage volume of normal lung with a radiation dose more than 20 Gy (V20 Gy), and normal tissue complication probability (NTCP), were calculated from DVH. The NTCP model of Lyman was used. In the NTCP model,

$$NTCP = 1/\sqrt{2\pi} \int_{-\infty}^{t} \exp(-t^2/2\,)dt \quad (1)$$

$$\mathrm{t} = (D - TD_{50}(v))/(m \times TD_{50}(v)) \quad (2)$$

$$v = V/V_{ref} \quad (3)$$

$$\mathrm{TD}\ (2) = \mathrm{TD}\ (\mathrm{v}) \times \mathrm{v}^{\mathrm{n}} \quad (4)$$

where TD50(v) is the 50% tolerance dose for uniform irradiation of the partial volume V. The partial- and whole-lung radiation tolerance doses were related by a power law relationship:

Where Vref is the volume of normal lung. The parameter n is the volume effect parameter, for which the value of 0.87 from the literature was applied. The parameter m is the steepness of the dose-complication curve for a fixed partial volume, and an estimate of 0.18 was used. The TD50 of 24.5 Gy was applied in the calculation. The effective-volume method of Kutcher and Burman was used to provide estimates of equivalent doses and volume pairs for uniform partial organ irradiation from the DVHs summarizing the non-uniform irradiation. The three parameters were derived according to Burman's identification: lung (TD50 = 24.5 Gy, n = 0.87, m = 0.18), heart (TD50 = 48.0 Gy, n = 0.35, m = 0.10) and spinal cord (TD50 = 66.5 Gy, n = 0.05, m = 0.175).

Statistical Analysis

Statistical analysis was carried out using the statistical software SPSS version 19.0. Data are expressed as mean ± standard deviation and were compared using the t-test. $P < 0.05$ was statistically significant.

RESULTS

Target and OAR Volume Changes

The mean volume change of the tumor target in 24 patients was 88.26% of the original volume on the CBCT image. CBCT automatically outlined the results, and the CT automatically outlined results were not very different. The results of the CBCT in the third patient showed an increase in volume, while the CBCT in the fifth patient showed a reduction in volume. Due to respiratory movement caused by the tumor target and the surrounding tissue movement, there was an error in the target of the radiotherapy and the plan target, resulting in changes in the dose.

The CBCT showed that the volume of the lungs changed relative to the fraction of treatment, and the volume of the lungs in most patients changed greatly with the fraction of treatment. The treated left and right lung were reduced to 93.39 and 96.79% of the original volume, respectively. At the end of treatment, the mean volume of the left and right lungs in 24 patients with CBCT images was 88.95 and 80.32% of the original volume, respectively. Comparison of CT and CBCT images showed the same changes in the left and right lung volumes. Besides the first case of a patient with a larger left lung volume, the remaining volumes were reduced. This shows that CBCT to analyze the pulmonary deformation of the registration was still more accurate and automatically showed that the method could better reflect the changes in lung volume.

Target and OAR Dose Changes

Figure 1 shows little change in CT and CBCT images with the fraction dose of the target. Most of the target volumes on the CT images and CBCT were not very different, and the impact on the dose was not large. The dose of PTV was not significantly different in any of the 24 patients, and the error was within 5%, indicating that the target was in a high-dose area during each fraction.

Figure 2 shows the change in CT and CBCT images with the fraction of dose to the OARs. The left and right lungs of 24 patients showed a substantially reduced lung volume and a mean increase in lung dose as a result of CT and CBCT calculation. The patient CBCT was used to sketch the results, and the left and right lung doses in the course of treatment were much greater than the CT image doses. The left and right lung CBCT

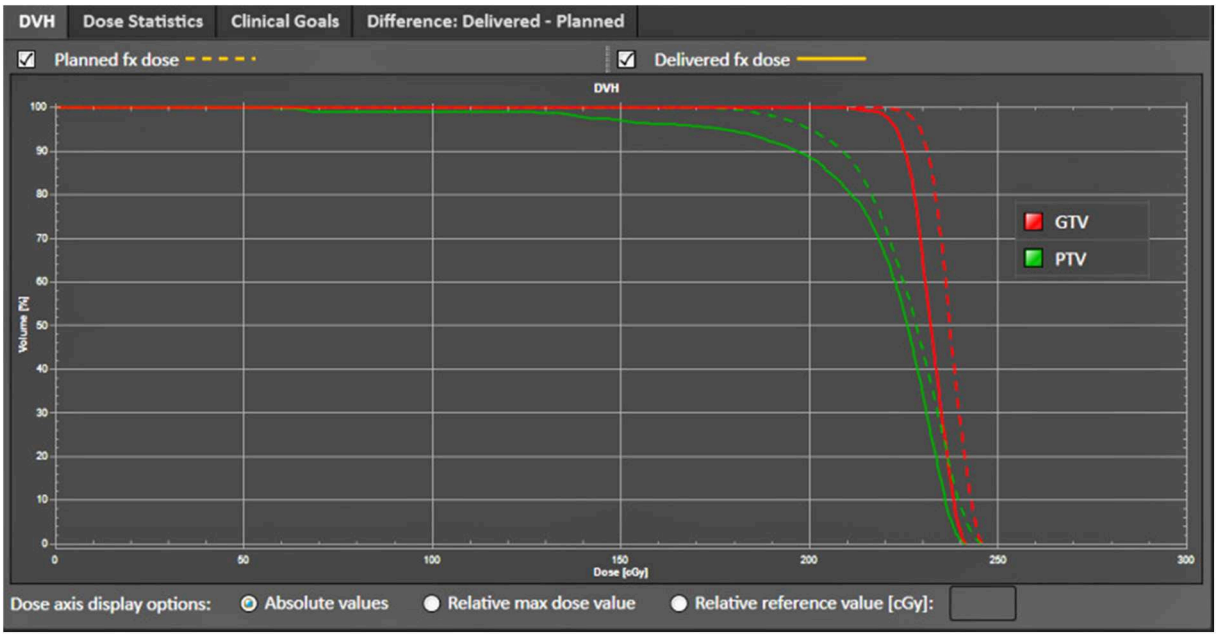

FIGURE 1 | DVH changes of the target area, the GTV and PTV.

of the 24 patients showed 167.31 ± 165.75 and 79.33 ± 54.11 cGy, respectively, and the cumulative dose was 164.63 ± 164.96 and 77.63 ± 53.36 cGy, respectively. Most of the 24 patients showed the same dose treatment progress, gradually decreased lung volume, and gradually increased lung dose, indicating that the reduction in lung volume and its dose increase have a certain relevance to whether the treatment at the original dose will cause excessive exposure.

Figure 3 shows the change in atelectasis on CT images with the fraction dose. There were four plans: Plan0327, Plan0403, Plan0410, and Plan0417. This patient had cT4N2M0 NSCLC and was treated with 30 fraction × 2.0 Gy. Two IGRT specialists, independent of each other, visually evaluated every MVCT. For each MVCT, the observed changes in atelectasis were scored. This result shows that it is very important to use image-guided radiotherapy (IGRT).

The Cumulative Dose Changes of Targets and OARs

Table 2 shows the cumulative dose of GTV D99. In addition to the first and fifth cases of patients with GTV, the cumulative dose was lower than the planned dose, but it was still within the clinical requirements to achieve the lowest dose. The other target did not show significant changes. No dose to the target showed any significant changes, indicating that the target had been under high dose coverage. In addition, there was no significant difference between CT and CBCT cumulative doses. When the target was reduced, we had to give the original target a sufficient dose to ensure the control rate of the tumor, indicating that the target was in the high-dose area.

The basic clinical information of the order, age, sex, and staging of 24 patients is shown in **Table 2**, and the volumes of GTV, PTV, left lung, and right lung as measured by CT images before treatment are listed.

Table 2 shows the results of GTV D95, D50, average, and PTV planned dose and cumulative dose changes and some evaluation parameters of the paired *t*-test analysis. The average dose changes yielded t values of 1.919, 2.299, 2.372, 2.197 in the course of treatment. The respective *P* values were 0.096, 0.055, 0.049, and 0.064. The CT plan and cumulative plan of the target PTV V100 reached the prescription dose of average volumes 95.59 and 81.47%. For GTV, the difference between planned dose and cumulative dose was statistically significant ($P < 0.05$).

Table 3 shows some of the differences in the assessment parameters of the lungs and the spinal cord and the difference between the planned dose and the applied cumulative dose. The cumulative dose to the lung and spinal cord in 24 patients decreased compared with the planned dose, and the cardiac Dmean accumulation showed an increase. Paired *t*-test analysis showed that the mean values of Dmean, left lung Dmean, heart Dmean, whole lung Dmean and spinal Dmax were 1.222, 0.480, −0.291, 0.786, and 1.683, respectively, and the *P* values were 0.261, 0.646, 0.780, 0.457, and 0.136, which were not statistically significant.

DISCUSSION

There are many important organs around a radiotherapy target. The control rate of lung cancer and the radiation therapy dose is related to the surrounding normal tissue dose limit and has become the biggest obstacle for conventional radiotherapy to

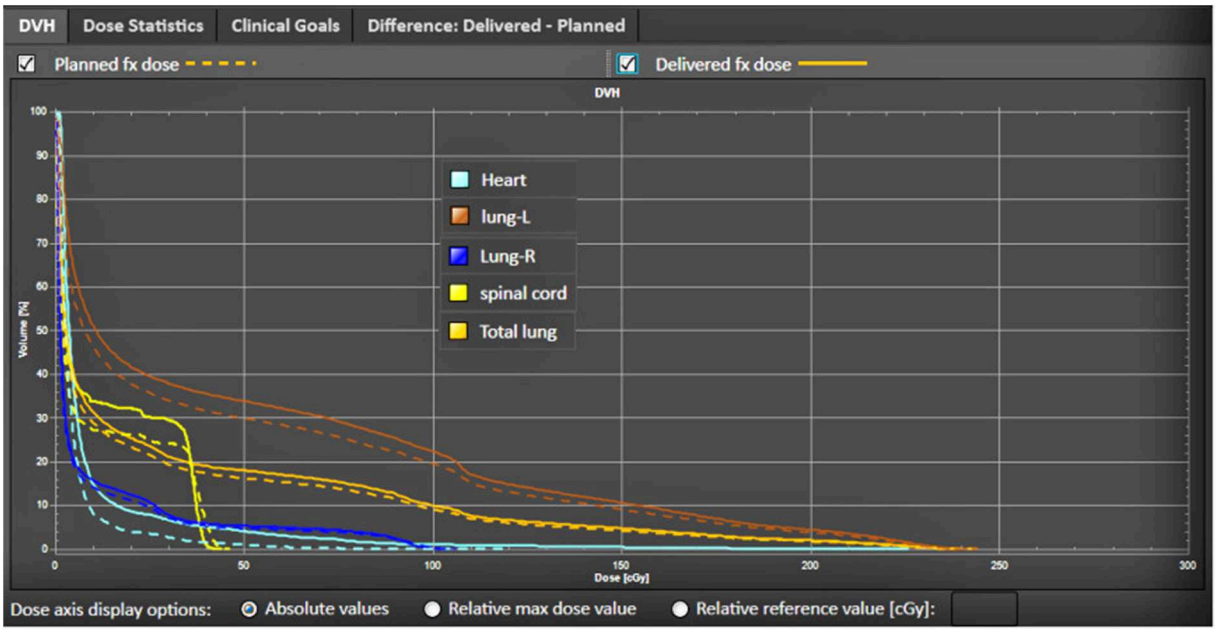

FIGURE 2 | DVH changes of the OARs, including the heart, spinal cord, and lungs.

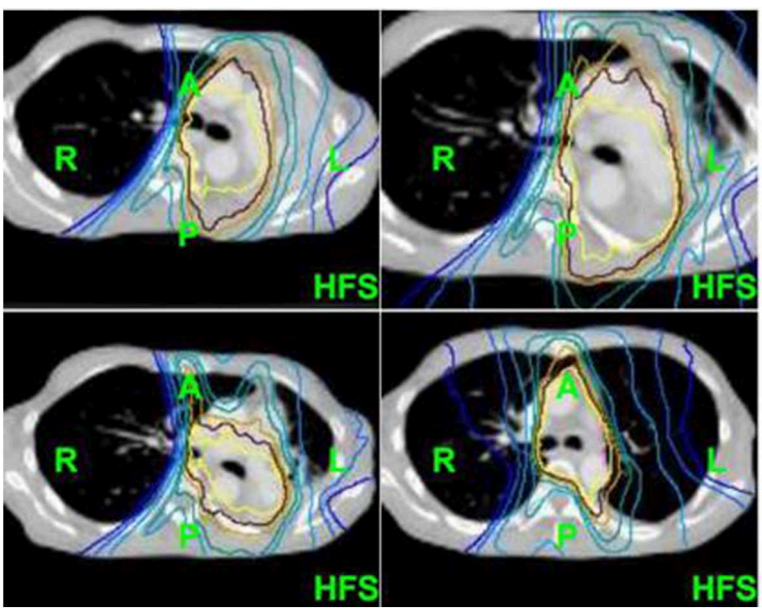

FIGURE 3 | The change in atelectasis on CT images with the fraction dose.

improve the tumor dose. CRT or IMRT radiotherapy can produce a dose distribution that is highly suitable for the shape of the target, reducing the surrounding normal tissue exposure and limiting the organ's dose, but from the pretreatment planning through the entire course of treatment [4], the dose distribution of the initial treatment plan changes during the actual treatment, and the difference between the administered dose and the planned dose is conducive to adjusting the radiotherapy plan for better and more accurate radiotherapy.

In this study, GTV Dmean decreased significantly during the course of treatment, indicating that the experience of the outgoing boundary may not have met the requirements. Kwong et al. [5] indicated that the results of the lung cancer GTV center for the displacement of the head and foot direction were

TABLE 2 | Differences in exposure dose between CT plan and accumulation plan.

GTV	CT plan	Accumulation plan	*t*-value	*P*-value
D_{95}	6179.00 ± 616.24	6156.35 ± 614.94	1.935	0.086
D_{50}	6308.90 ± 656.02	6662.25 ± 629.93	2.467	0.067
Average	6307.45 ± 624.22	5753.90 ± 630.27	2.254	0.039
PTV (V_{100})	96.59 ± 2.29%	89.67 ± 18.71%	2.456	0.067

TABLE 3 | Differences in organs-at-risk dose between CT plan and accumulation plan.

Organs (Gy)	CT plan	Accumulation plan	*t* value	*P* value
Right lung D_{mean}	793.30 ± 54.11	776.3 ± 53.36	1.222	0.261
Left lung D_{mean}	1673.10 ± 165.75	1646.3 ± 164.96	0.480	0.646
Heart D_{mean}	618.80 ± 66.70	683.8 ± 60.91	−0.291	0.780
Total lung D_{mean}	1181.40 ± 67.22	1158.7 ± 66.19	0.786	0.457
Spinal cord D_{max}	3726.20 ± 185.91	3600.0 ± 173.14	1.683	0.136
NTCP of right lung (%)	1.60 ± 0.74	1.33 ± 0.86	1.702	0.085
NTCP of left lung (%)	6.00 ± 1.94	5.34 ± 1.76	0.897	0.124
NTCP of heart (%)	4.77 ± 2.15	4.55 ± 2.37	−0.532	0.112
NTCP of total lung (%)	2.53 ± 1.32	1.95 ± 1.22	1.023	0.075
NTCP of spinal-cord (%)	2.03 ± 0.72	1.81 ± 0.94	1.224	0.090

significantly smaller than those of the corresponding direction of the diaphragm. Therefore, the expansion of the safety boundary according to experience may cause excessive exposure of normal tissue. PTV reached as low as 81.47% of the prescribed dose volume. In three selected middle esophageal cancer patients with three-dimensional conformal radiotherapy, Brown et al. [6] illustrated the need to replan during the course of treatment.

Replanning should be done only at the right time. Ding et al. [7] studied 87 patients with IMRT and three-dimensional adaptive radiotherapy, followed by 18F-FDG PET/CT scans after 40 Gy irradiation, and mapped the target. Zhang et al. [8] studied 40 cases of NSCLC radiotherapy target volume changes. Comparing the number of irradiations $\leq$ 20 times the reset and 20 times after the reduction of the GTV reduction ratio and Dmean decline ratio in the ipsilateral lung and whole lung, they concluded that 40 Gy/20 replanning is the most reasonable, but different individuals should be differentially planned using PET and CT fusion images. The tumors subsided significantly in their patients.

Because the soft-tissue contrast of CT images is high, the soft-tissue contrast of CBCT is poor. In a previous study, we used CT scanning to repeat the changes that doctors made in target and normal tissues. In this study, we used CT and multiple CBCT to outline the results. The lungs and target changed as the treatment progressed, and to varying degrees. CBCT images were used to outline the tumors. The lungs and spinal cord permitted a better sketch effect, and for targets with a low surrounding tissue contrast, the algorithm still needs to continue to be improved [9]. The image algorithm mainly includes the frequency domain Contourlet transform, wavelet transform and spatial domain non-local mean filtering [10–12]. These algorithms have much room for development.

By the use of deformation registration, we can outline the CT image profile to the kilovolt-like CBCT image, decomposed into multiple CBCT calculations, and the CBCT dose is added each time. The total dose will be transplanted to the planning CT image. The obtained results will reduce the patient position changes, organ volume changes, and other uncertain factors. The results of dose uptake using CBCT showed that there was some difference between the delivered dose and the planned dose during the treatment of the lungs, while the dose to the heart increased and the dose to the spinal cord decreased slightly. More cases are needed to supplement the data and confirm the conclusions of this study.

Since we need to superimpose each dose on the original CT and compare it with the planning CT, we need to calibrate the CBCT's HU-RED table accurately to obtain a more accurate cumulative dose [13]. In this study, we used RayStation software to automatically divide the HU values by the different tissue densities. The accuracy of the method was improved compared to the traditional method of calibration. Another method is to map the ROIs between CT and CBCT, but due to positioning errors and CBCT image quality, these two methods cannot completely eliminate the error [14–19], but they can meet the current clinical requirements.

In summary, this NSCLC radiotherapy target and an OAR real DVH preliminary study was based on the offline artificial correction method, and the process took much more time. In addition, whether the accuracy of the two image target regions and normal tissue deformation registration affects the calculation of DVH parameters remains to be verified. By improving the speed and accuracy of deformation registration, we can achieve rapid online correction of radiotherapy targets and adaptive radiotherapy.

CONCLUSION

The doses to the lung and to other normal organs did not change much, and there was no statistically significant difference in the probability of complications in normal tissues. However, in some patients, the radiation dose in the target area was reduced, which may have led to missed targets.

DATA AVAILABILITY STATEMENT

The datasets generated for this study are available on request to the corresponding author.

ETHICS STATEMENT

This study was carried out in accordance with the recommendations of Ethics Committee Approval at Shandong Cancer Hospital and Institute. The protocol was approved by Ethics Committee of the Shandong Cancer Hospital and

Institute. As the study is retrospective, the need for written informed consent from participants was waived.

AUTHOR CONTRIBUTIONS

JL and CdM drafted conception and design and draft the manuscript. ZL and CsM contributed to acquire, analyze, and interpret data. SY contributed to acquire data and enhanced its intellectual content. All authors read and approved the final manuscript.

FUNDING

This work was supported by Natural Science Foundation of Shandong Province (ZR2019MH136, ZR2017BA024), Projects of Medical and Health Technology Development Program in Shandong Province (2017WS110, 2017WS306), Project funded by China Postdoctoral Science Foundation (2019M652356), The National Nature Science Foundation of China (81800156, 81974467).

REFERENCES

1. Endo M, Tsunoo T, Kandatsu S, Tanada S, Aradate H, Saito Y. Four-dimensional computed tomography (4D CT)–concepts and preliminary development. *Radiat Med*. (2003) **21**:17–22.
2. Zhao JD, Xu ZY, Zhu J, Qiu JJ, Hu WG, Cheng LF, et al. Application of active breathing control in 3-dimensional conformal radiation therapy for hepatocellular carcinoma: the feasibility and benefit. *Radiother Oncol*. (2008) **87**:439–44. doi: 10.1016/j.radonc.2007.12.006
3. Ma C, Hou Y, Li H, Li D, Zhang Y, Chen S, et al. A Study of the anatomic changes and dosimetric consequences in adaptive CRT of non-small-cell lung cancer using deformable CT and CBCT image registration. *Technol Cancer Res Treat*. (2014) **13**:95–100. doi: 10.7785/tcrt.2012.500365
4. Xi M, Liu MZ, Deng XW, Zhang L, Huang XY, Liu H, et al. Defining internal target volume (ITV) for hepatocellular carcinoma using four-dimensional CT. *Radiother Oncol*. (2007) **84**:272–8. doi: 10.1016/j.radonc.2007.07.021
5. Kwong Y, Mel AO, Wheeler G, Troupis JM. Four-dimensional computed tomography (4DCT): a review of the current status and applications. *J Med Imaging Radiat Oncol*. (2015) **59**:545–54. doi: 10.1111/1754-9485.12326
6. Brown E, Owen R, Harden F, Mengersen K, Oestreich K, Houghton W, et al. Head and neck adaptive radiotherapy: predicting the time to replan. *Asia Pac J Clin Oncol*. (2016) **12**:460–7. doi: 10.1111/ajco.12516
7. Ding X, Li H, Wang Z, Huang W, Li B, Zang R, et al. A clinical study of shrinking field radiation therapy based on F-18-FDG PET/CT for stage III non-small cell lung cancer. *Technol Cancer Res Treat*. (2013) **12**:251–7. doi: 10.7785/tcrt.2012.500310
8. Zhang YJ, Li JB, Lu J, Liu TH, Gong GZ, Ma CS, et al. Study on modification of radiotherapy plan for three dimensional conformal radiotherapy for non small cell lung cancer. *Chin J Cancer Prev Treat*. (2010) **17**:1852–4.
9. Dobashi S, Sugane T, Mori S, Asakura H, Yamamoto N, Kumagai M, et al. Intrafractional respiratory motion for charged particle lung therapy with immobilization assessed by four-dimensional computed tomography. *J Radiat Res*. (2011) **52**:96–102. doi: 10.1269/jrr.10019
10. Chen X, Gilkeson RC, Fei B. Automatic 3D-to-2D registration for CT and dual-energy digital radiography for calcification detection. *Med Phys*. (2007) **34**:4934–43. doi: 10.1118/1.2805994
11. Lu X, Zhang S, Su H, Chen Y. Mutual information-based multimodal imageregistration using a novel joint histogram estimation. *Comput Med Imaging Graph*. (2008) **32**:202–9. doi: 10.1016/j.compmedimag.2007.12.001
12. Ren L, Godfrey DJ, Yan H, Wu QJ, Yin FF. Automatic registration between reference and on-board digital tomosynthesis images for positioning verification. *Med Phys*. (2008) **35**:664–72. doi: 10.1118/1.2831903
13. Ma C, Cao J, Yin Y, Zhu J. Radiotherapy dose calculation on KV cone-beam CT image for lung tumor using the CIRS calibration. *Thorac Cancer*. (2014) **5**:68–73. doi: 10.1111/1759-7714.12055
14. Nithiananthan S, Brock KK, Daly MJ, Chan H, Irish JC, Siewerdsen JH. Demons deformable registration for CBCT-guided procedures in the head and neck: convergence and accuracy. *Med Phys*. (2009) **36**:4755. doi: 10.1118/1.3223631
15. Wang H, Dong L, O'Daniel J, Mohan R, Garden AS, Ang KK, et al. Validation of an accelerated'demons' algorithm for deformable image registration in radiation therapy. *Phys Med Biol*. (2005) **50**:2887. doi: 10.1088/0031-9155/50/12/011
16. Lou Y, Niu T, Jia X, Vela PA, Zhu L, Tannenbaum AR. Joint CT/CBCT deformable registration and CBCT enhancement for cancer radiotherapy. *Med Image Anal*. (2013) **17**:387–400. doi: 10.1016/j.media.2013.01.005
17. Yu G, Liang Y, Yang G, Shu H, Li B, Yin Y, et al. Accelerated gradient-based free form deformable registration for online adaptive radiotherapy. *Phys Med Biol*. (2015) **60**:2765–83. doi: 10.1088/0031-9155/60/7/2765
18. Li N, Zarepisheh M, Uribe-Sanchez A, Moore K, Tian Z, Zhen X, et al. Automatic treatment plan re-optimization for adaptive radiotherapy guided with the initial plan DVHs. *Phys Med Biol*. (2013) **58**:8725–38. doi: 10.1088/0031-9155/58/24/8725
19. Zarepisheh M, Long T, Li N, Tian Z, Romeijn HE, Jia X, et al. A DVH-guided IMRT optimization algorithm for automatic treatment planning and adaptive radiotherapy replanning. *Med Phys*. (2014) **41**:061711. doi: 10.1118/1.4875700

Conflict of Interest: The authors declare that the research was conducted in the absence of any commercial or financial relationships that could be construed as a potential conflict of interest.